Heliyon 6 (2020) e03865

Contents lists available at ScienceDirect

Heliyon

journal homepage: www.cell.com/heliyon

Research article

Thermal stability of human matrix metalloproteinases

Noemi Meraz-Cruz [a,b], Felipe Vadillo-Ortega [a,b], Aura M. Jiménez-Garduño [a,c], Alicia Ortega [a,*]

[a] Department of Biochemistry, Faculty of Medicine, Universidad Nacional Autónoma de México, 04510, Mexico City, Mexico
[b] UNAM School of Medicine Branch, National Institute of Genomic Medicine, Mexico
[c] Health Sciences Department, School of Sciences, Universidad de Las Americas Puebla, San Andrés Cholula Puebla CP72810, Puebla, Mexico

ARTICLE INFO

Keywords:
Chemistry
Biological sciences
Proteins
Biochemistry
Metalloproteinases
Stromelysin
Collagenase
Matrilysin
Protein denaturation
Differential scanning calorimetry

ABSTRACT

Matrix metalloproteinases (MMP) are key players in the remodelling of the extracellular matrix under physiological and pathological conditions. Thermodynamic parameters of human recombinant metalloproteinases of the active (rMMP2, 3, 7, 8 and 9) and latent (rPro-MMP2, 3 and 9) forms were obtained by differential scanning calorimetry (DSC). Temperature by itself does not result in autocatalysis of recombinant MMP. The transitions observed by DSC correspond to structural domains of the monomeric protein. In this study, we show the domain organization of these proteins, where the thermal transition (Tm) of the main component is observed at 71.3 °C (ProMMP-2); 74.8 °C (ProMMP-8); 80.0 °C (ProMMP-3); 92.6 °C (ProMMP-9) and 98.3 °C (ProMMP-7). For MMP-3, this main Tm is related to the catalytic domain (CD). The isolated recombinant CD of MMP-3 unfolds as a single transition at Tm 83.4 °C, matching the more stable domain observed in the full-length active form of rMMP-3. The denaturation profile of rProMMP-3 shows the main transition at Tm 80 °C, a less stable domain before the propeptide domain (PD) cleavage. Our results indicate that the structural stability of MMP and particularly their CD are not substantially altered after cleavage of the PD. We propose that the thermodynamic parameters obtained by DSC are relevant for the functional study of MMP, particularly to reveal their contribution in complex biological samples in health and disease.

1. Introduction

Matrix metalloproteinases (MMP) are a group of zinc-dependent enzymes responsible for degradation of the extracellular matrix components in normal events such as embryogenesis [1], fetal membrane rupture during delivery [2], implantation [3], as well as in many pathological processes [4]. The MMP family members differ in their molecular weight, structural domain organization, substrate specificity, and regulation of functions [5]. The MMP are characterized by conserved functional and structural domains, such as the signal peptide, the propeptide domain (PD), the catalytic domain (CD), which contains the Zn^{2+}-binding site [6], and the hemopexin domain (HD) [5]. All family members which are secreted as zymogens have a sequence of about 10 kDa (PD), which must be removed upon activation. There are however, membrane type MMPs (MT-MMPs), which share a common domain structure consisting of a signal peptide, a PD, CD, a hemopexin-like (HD) domain, a hinge (linker-1) and a stalk region (linker-2) [7]. In MMP, the proenzyme structure is maintained by the binding of Zn^{2+} to a conserved cysteine (Cys) residue located in a Cys switch motif <PRCGXPD> present in the PD. The Cys-Zn^{2+} interaction can be released by physical (chaotropic agents), chemical (HOCl, mercurials), or enzymatic (trypsin, plasmin) [8] treatments that result in the separation of the Zn^{2+} from the Cys residue leading to activation of the enzyme. The activity of MMP is tightly regulated due to their potential impact on the extracellular matrix degradation and tissue integrity. Structural and functional characteristics of these enzymes are compared and summarized in Table 1. The MMP structure has been studied by different techniques [9, 10], in the present study we analysed the thermodynamic parameters of rMMP from thermal denaturation to further understand the stability and domain organization of some representative members of this enzyme family, considering as representatives three of the four MMP subgroups, i.e., the interstitial collagenases (MMP-8), stromelysins (MMP-3), matrilysin (MMP-7), and gelatinases (MMP-2 and MMP-9). Differential scanning calorimetry (DSC) was used to investigate protein stability, which is directly related to protein structure and conformation [11]. Many factors are responsible for the folding and stability of native proteins, including hydrophobic interactions, hydrogen bonds, conformational entropy, and the physical environment. The T_m obtained from the DSC protein denaturation profile is an indicator of protein thermal stability, where a higher T_m means the protein is more stable. Enthalpy is determined by the integral of the ΔCp,

* Corresponding author.
E-mail address: aortega@unam.mx (A. Ortega).

https://doi.org/10.1016/j.heliyon.2020.e03865
Received 18 October 2019; Received in revised form 20 February 2020; Accepted 23 April 2020

Table 1. Characteristics of MMP involved in extracellular matrix degradation.

	Alternative Name	Molecular weight (kDa)		Molecular structure
		Proenzyme	Active enzyme	
MMP-1 (P03956)	Interstitial collagenase	54007	43000	
MMP-2 (P08253)	Collagenase IV, Gelatinase A	73882	65000	
MMP-3 (P08254)	Stromelysin 1, roteoglycanase, Transin	53977	45000	
MMP-7 (P09237)	Matrilysin, Matrin	29677	19000	
MMP-8 (P22894)	Neutrophil collagenase	53412	44000	
MMP-9 (P14780)	Collagenase V, Gelatinase B	92000	83000	

Domain arrangements:
Signal peptide; Fibronectin type domain; Linker region.
Propeptide; Collagen-like domain.
Catalytic domain; Hemopexin-like domain.

which is obtained directly by DSC data. The rationale for this approach is to look for new tools to explore the biochemistry and biology of these enzymes, considering their thermal stabilities and their importance in health and disease.

2. RESULTS

For all rMMP used, a single protein band was present of the recombinant, as determined by SDS-PAGE, except for rMMP-9, which showed two bands. For SDS-PAGE, proteins were temperature denatured and no proteolysis during heating was observed.

2.1. Denaturation profile recombinant gelatinase A (MMP-2)

Figure 1A, shows the immunoblot of recombinant gelatinase A. With a band at 74 kDa corresponding to rPro-MMP-2 and a band at 65 kDa corresponding to rMMP-2, as previously reported [12]. Figure 1B, represents the predicted protein structures for Pro-MMP-2 and MMP-2. Full length ProMMP-2 contains all four domains; PD (Red ribbons), CD (Green ribbons), HD (Blue ribbons) and FD (fibronectine-like domain) (Yellow ribbons). Removal of the PD from rPro-MMP-2 yields a protein with different conformation, however, the conformations of HD and CD are conserved, as it is shown by the predicted structure. Figure 1C, shows the denaturation profile of rPro-MMP-2 and rMMP-2. After baseline correction, the denaturation profile for rPro-MMP-2 (upper case) shows two transitions, which unfold at T_m (I) 54.1 °C and T_m (II) 71.3 °C, indicating two structural domains that may have strong co-operative interactions, as it has been proposed to occurred for other monomeric proteins where the denaturation profiles yield more than one transitions [13, 14]. Active rMMP-2 (lower case), denatures as a single broad transition with average T_m (I) 67.5 °C. However, a second transition included in the broad transition can be fitted at T_m (II) 78 °C. The enthalpy contributions of rPro-MMP2 and rMMP-2 are similar, as can be seen in Table 2.

2.2. Denaturation profile recombinant Stromelysin (MMP-3)

Figure 2A shows the immunoblot of recombinant Stromelysin, 54 and 45 kDa (rPro-MMP-3 and rMMP-3 respectively, as has been previously

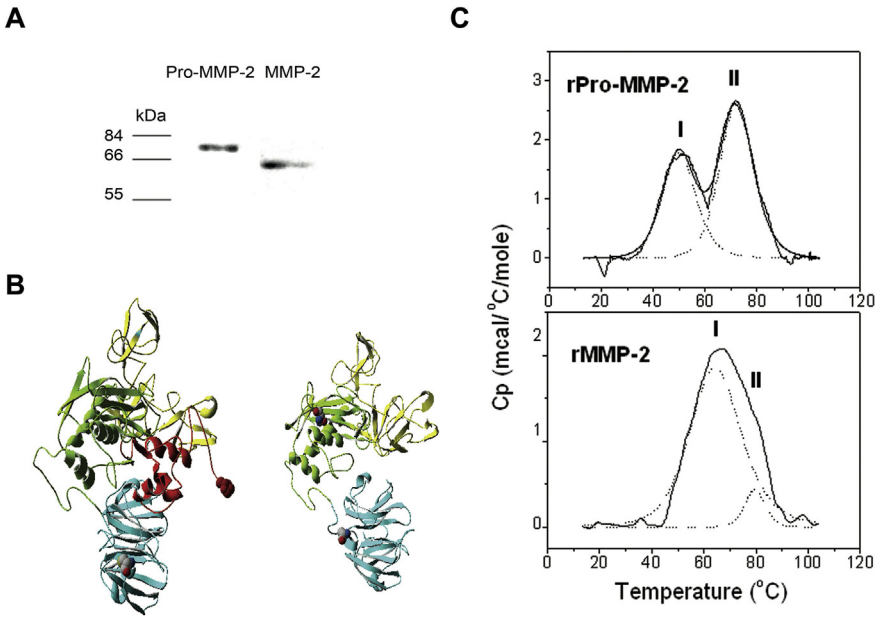

Figure 1. Analysis of rProMMP-2 and rMMP-2 structures. A) Immune-reactivity of anti MMP-2 antibody with the recombinant Pro-MMP-2 and MMP-2. B) Predicted model for ProMMP-2 (protein modelling based on SWISSPROT No. P08253). Blue ribbon is related to the C-terminal-Hemopexin domain (HD). Green ribbons are related with the N-terminal-catalytic domain (CD). Red ribbon is related to the pro-peptide domain, which is removed upon activation. Yellow ribbon is associated with the fibronectin-like domains (FD). C) DSC profiles of excess Cp as a function of increasing temperature of rPro-MMP-2 (upper panel) and rMMP-2 (lower panel): Experimental data (solid line curve) and best theoretical fit (dotted line curves), with transitions temperatures, labelled I and II.

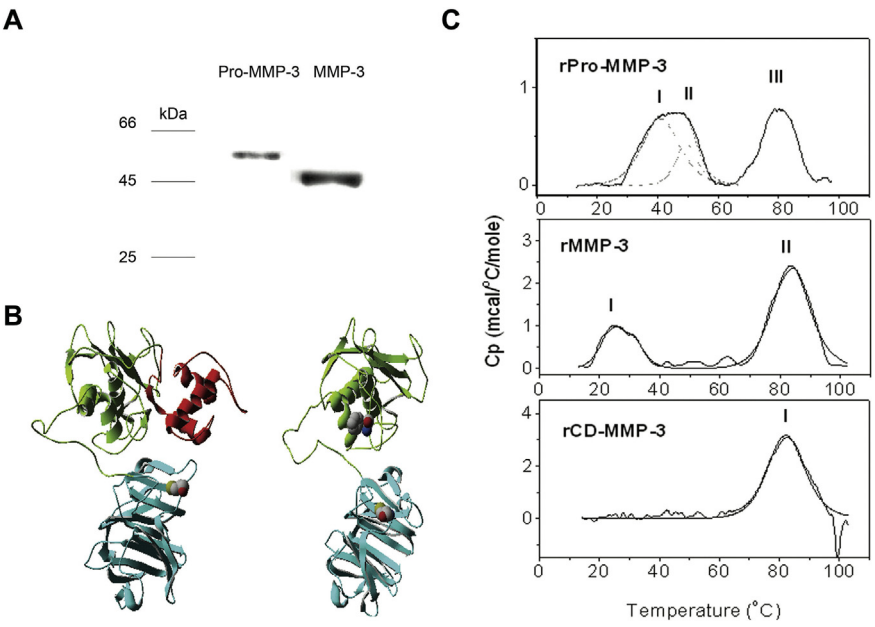

Figure 2. Analysis of rMMP-3 structure. A) Immunereactivity of anti MMP-3 antibody with the recombinant Pro-MMP-3 and MMP-3. B) Predicted model for rProMMP-3 (protein modelling based on SWISSPROT No. P08254). Blue ribbon is related to the C-terminal Hemopexin domain. Green ribbon is related with the N-terminal Catalytic domain. Red ribbon is related to the pro-peptide domain (PD), which is removed upon enzyme activation. C) DSC profiles of excess Cp as a function of temperature of rPro-MMP-3 (upper panel); rMMP-3 (middle panel) and rCD-MMP3 (lower panel). Experimental data (solid line curve) and best theoretical fit (dotted line curves) with transitions temperatures, labelled I, II, and III.

reported [17]. Figure 2B represents the predicted protein structure for rPro-MMP-3 with the PD (Red ribbons), the HD (Blue ribbons) and CD (Green ribbons). Removal of the PD to yield rMMP-3 conserves the conformation for the predicted CD structure. Figure 2C, shows the denaturation profile of rProMMP-3, rMMP-3 and the isolated catalytic domain rCD of MMP-3. The denaturation profile of rPro-MMP-3 has three defined transitions at T_m (I) 41.2 °C, (II) 45.7 °C and (III) 80 °C (upper case) and the active rMMP-3 shows two transitions at T_m (I) 26.4 y (II) 83.9 °C (Middle case). The unfolding profile of the rCD has a single transition observed at T_m (I) 83.4 °C (lower case). The T_m of rCD is also present in rMMP-3 and in rProMMP-3, indicating that the CD is more stable and structurally independent from the rest of the protein. The enthalpy contribution of each transition is listed in Table 2.

2.3. Denaturation profile of recombinant Matrilysin (MMP-7)

Figure 3A, shows the SDS-PAGE of recombinant Matrilysin, the active form of rMMP-7. A single protein band was observed at 19 kDa, as previously reported for MMP-7 [18]. Figure 2B, represents the CD (Green ribbons) of the predicted protein structure for the smallest member of the MMP family, when compared with MMP-2 and MMP-3. Figure 3C, shows the denaturation profile of rMMP-7, which denatures as a single sharp transition at T_m 98.3 °C, the highest thermal stability observed among all rMMP analysed in this study. The rMMP-7 unfolds with a lower enthalpy compared with the rest of rMMP, see Table 2. Due to the high thermal stability of rMMP-7 it could be possible to relate the denaturation of the full-length rMMP-7 to the structure corresponding to the CD in other MMP.

2.4. Denaturation profile of recombinant MMP-8

Figure 4A, shows the immunoblot of the active rMMP-8 with a single band of 54 kDa, as has been reported [19]. Figure 4B, represents the predicted protein structure of the active form, where the HD (Blue ribbons) and CD (Green ribbons) represent the two separated structural domains predicted for this protein. Figure 4C shows the denaturation profile of rMMP-8, where two transitions are observed at T_m (I) 32 °C and (II) 74.8 °C. The enthalpy contribution of component II, is like that observed for the transition of higher T_m obtained for the other MMP studied, see Table 2.

2.5. Denaturation profile of recombinant MMP-9

Figure 5A, shows the immunoblot of anti-MMP-9 as a single protein of 92 kDa, which corresponds to recombinant Pro-MMP-9 [20]. However, the active form of the protein rMMP-9 showed two bands [21], in this study, 56% corresponded to the 83 kDa protein as has been previously reported, which results from MMP-2 cleavage [21], and 44% of the rMMP-9 sample, has a 65 kDa protein, which has been also previously reported to result from MMP-3 cleavage [22]. Figure 5B, represents the predicted protein structures for Pro-MMP-9 and MMP-9. Full length ProMMP-9 contains all four domains; PD (Red ribbons), CD (Green ribbons), HD (Blue ribbons) and FD (Yellow ribbons). Removal of the PD from rPro-MMP-2 yields a protein with different conformation, however, the conformations of HD and CD are conserved, as it is shown by the predicted structure. Figure 5C shows, the denaturation profile of the

Table 2. Thermodynamic parameters of the recombinant MMPs irreversible unfolding.

MMP	Peak	Tm (°C)	ΔH (kJ/mole)
ProMMP-3	I	41.2 ± 0.13	103.76
	II	45.7 ± 0.18	157.70
	III	80.0 ± 0.05	180.44
Active MMP-3	I	26.4 ± 0.55	172.00
	II	83.9 ± 0.06	117.90
CD-MMP-3	I	83.4 ± 0.15	223.00
ProMMP-2	I	54.1 ± 0.08	129.19
	II	71.3 ± 0.05	188.67
Active MMP-2	I	69.7 ± 0.22	182.01
	II	77.6 ± 0.29	76.9
Active MMP-7	I	98.3 ± 0.27	57.73
Active MMP-8	I	32.0 ± 0.02	24.68
	II	74.8 ± 0.37	229.70
ProMMP-9	I	92.6 ± 0.04	233.04
Active MMP-9	I	30.9 ± 0.15	24.26
	II	40.7 ± 0.39	94.97
	III	76.1 ± 0.04	592.45

Tm and ΔH correspond to the theoretical fit (n = 2), refer to the absolute error of mean (±AEM) of two different runs.

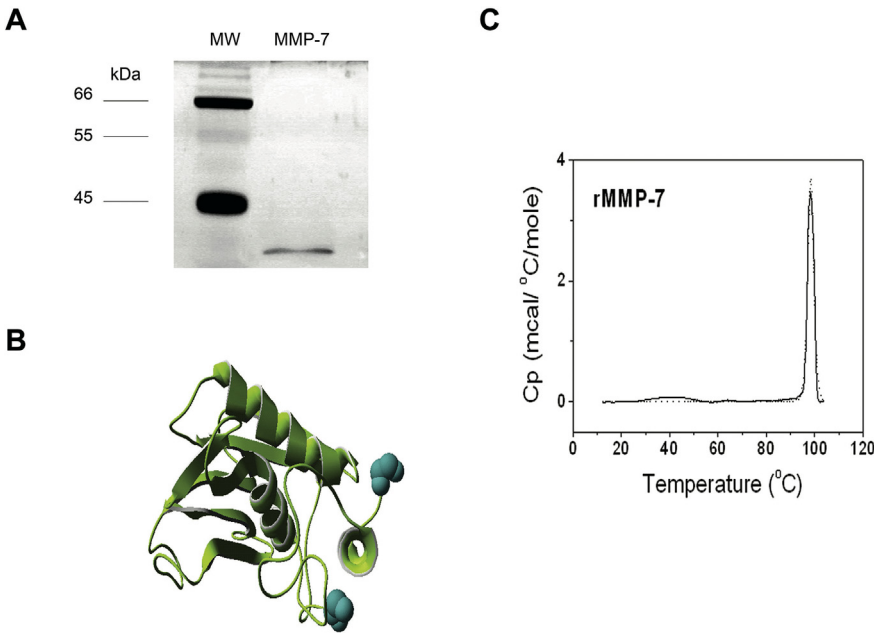

Figure 3. Analysis of rMMP-7 structure. A) SDS-PAGE of rMMP-7 determined by silver staining as described under Material and Methods. B) Predicted model for ProMMP-7 (protein modelling based on SWISSPROT No. P09237). MMP-7 is the catalytic domain represented by green ribbon in the rest of the MMP. C) DSC denaturation profiles of rMMP-7, excess Cp as a function of increasing temperature. Experimental data (solid line curve) and best theoretical fit (dotted line curves).

rPro-MMP-9 (upper case) with a single transition T_m 92 °C, whereas the denaturation profile of the rMMP-9 shows three transitions at T_m (I) 31 °C, (II) 41 °C and (III) 76 °C. Although it seems like the contribution of the proteins detected as rMMP-9 in the immunoblot are almost of the same proportion, the denaturation profile reveals three uneven enthalpy contributions of the observed transitions. The enthalpy contribution of rMMP-9 component III, is two-fold higher in comparison to the related component (CD) of rMMP-2, rMMP-3, and rMMP-8 (see Table 2), suggesting that the two proteins observed by immunoblot for rMMP-9, may unfold under the same transition.

2.6. Correlation between DSC denaturation profile parameters and structural characteristics

After calculating thermodynamic parameters from DSC for each metalloproteinase analysed in this study, we aimed to correlate those

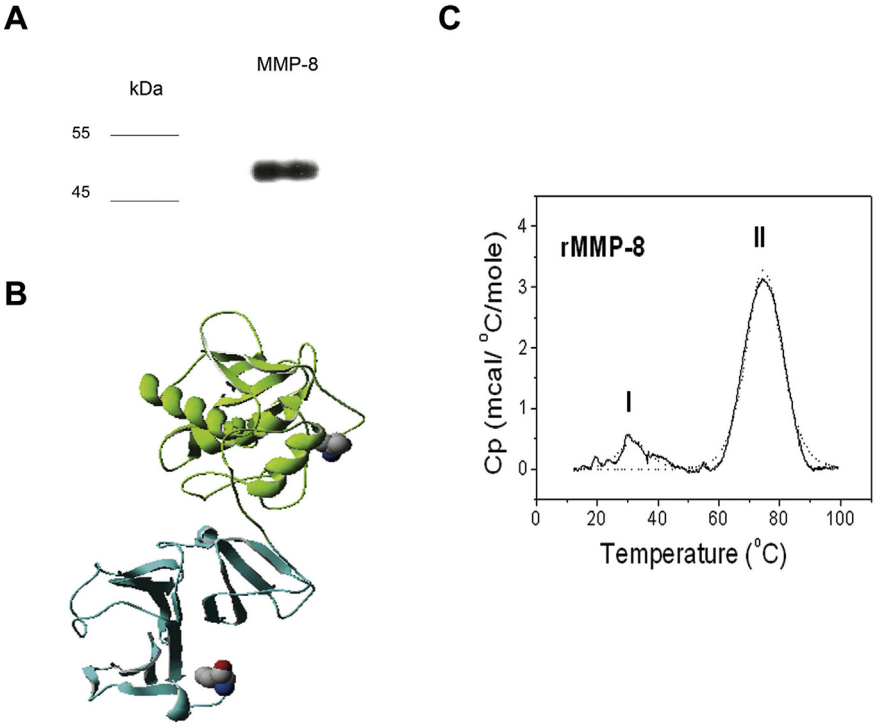

Figure 4. Analysis of rMMP-8 structure. A) SDS-PAGE of rMMP-8. B) Predicted model for ProMMP-8 (protein modelling based on SWISSPROT No. P22894). Blue ribbon is related to the C-terminal Hemopexin domain. Green ribbon is related with the N-terminal, catalytic domain. C) DSC profiles of excess Cp as a function of temperature of rPro-MMP-8. Experimental data (solid line curve) and best theoretical fit (dotted line curves).

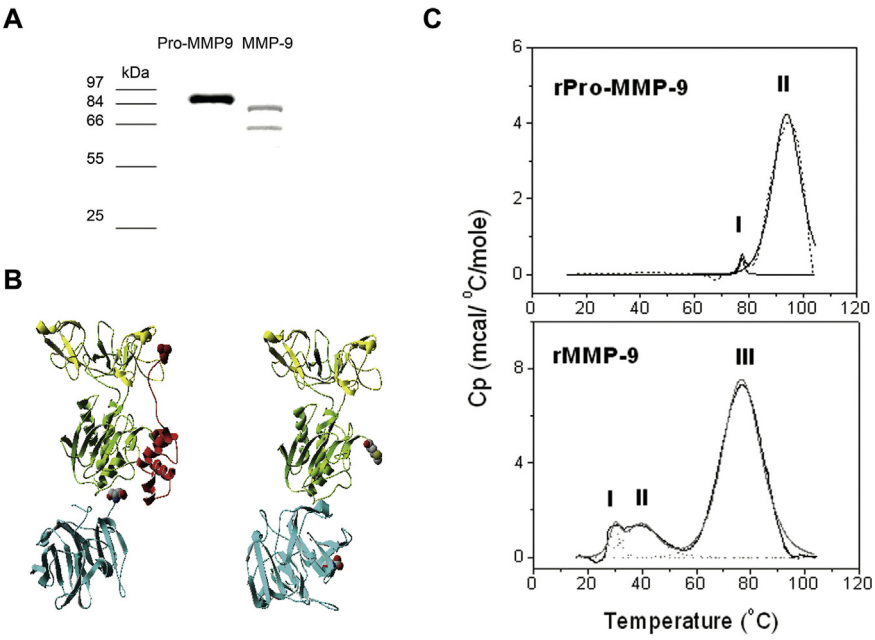

Figure 5. Analysis of rMMP-9 structure. A) Immunereactivity of anti MMP-9 antibody to recombinant Pro-MMP-9 and MMP-9. B) Predicted model for Pro-MMP-9 (protein modelling based on SWISSPROT No. P14780). Blue ribbon is related to the C-terminal Hemopexin domain. Green ribbon is related with the N-terminal catalytic domain. Red ribbon is related to the pro-peptide domain, which is removed upon activation. Yellow ribbon is related to the fibronectin-like domains. C) DSC profiles of excess Cp as a function of increasing temperature, for rPro-MMP-9 (upper panel) and rMMP-9 (lower panel). Experimental data (solid line curve) and best theoretical fit (dotted line curves).

parameters with other structural ones that could explain the differences in protein stability. Figure 6 shows that if ordered by molecular weight, MMPs could be nicely fitted into graphs describing their thermodynamic properties. MMP-7 is the smallest molecule analysed which showed the highest Tm value, and lowest ΔH. These values are attributable to a very high degree of protein stability (high Tm), and flexibility (low ΔH) [23]. If we calculate C_{pTm} (C_p at T_m) of each active form of MMP using Kirchhoffs law ($C_p = \Delta H/\Delta T$) we can attribute a specific C_{pTm} value to each metalloproteinase. In the case of MMP-7 the value is below one ($C_{pTm} = 0.59$). MMP-7 is also known to belong to the "shallow" S_1' pocket MMP type. S_1' pocket belongs to the selectivity region of the catalytic domain and its geometry and electrostatic features are key players for inhibitors design [24], here we found that our correlation and C_{pTm} value also distinguishes between the S_1' pocket MMP type. A shallower pocket could be associated to a more stable conformation since it has fewer gaps between atoms. In the case of MMP-3 classified as a "deep" S_1' pocket, C_{pTm} increases to 1.4, deeper pockets are surely associated to some degree of "less stable" conformations, and we found it correlated to a lower T_m and higher ΔH, compared to MMP-7. Finally, all the members of the "intermediate" S_1' pocket show C_{pTm} values over 2 (MMP-8 $C_{pTm} = 3$; MMP-2 $C_{pTm} = 2{,}65$; MMP-9 $C_{pTm} = 7{,}79$) and showed the lower T_m values.

3. DISCUSSION

The catalytic activity of MMP is a temperature-dependent processes, which have been previously described for MMP-9, MMP-1 and MMP-3 [25, 26, 27]. There are no evidences, including the present results, which indicate a temperature-dependence activation for auto proteolytic activity of any of the MMP used in this study. Heating rProMMP or rMMP at a rate 1 °C/min up to 95 °C for SDS-PAGE analysis, did not result in proteolysis in any of the MMP tested. Therefore, the different transitions observed during the thermal denaturation of a monomeric MMP, are associated to different structural domains. There are many examples of protein denaturation of human enzymes and enzymes from other mammals, where Tm is over 50 °C [14, 28]. Membrane proteins with enzymatic activity unfold at much lower temperatures especially in mammals [29], for example, SERCA1, has a Tm at 49–50 °C, a protein which we have been working more extensively [15, 30].

In this study, we observed important modifications in the thermodynamic parameters of proenzyme and active forms of MMP; 1) The predicted structures for active and inactive forms of MMP, did not present major changes in the structures related to the HD and CD after the removal of the PD fragment. 2) Pro-MMP and MMP shown a well-defined structural domain, with a high T_m over 70 °C.

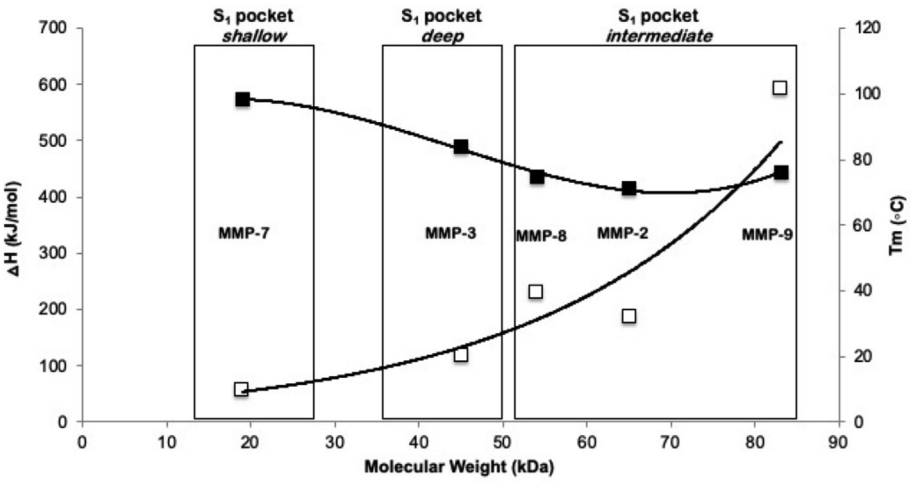

Figure 6. Correlation between molecular weight and thermodynamic DSC parameters. Black squares correspond to T_m (°C) axis and white squares correspond to ΔH (kJ/mol) axis. For T_m series, a polynomial regression was performed ($y = 0,0004 \times 3 - 0,0529 \times 2 + 1,4952x + 86,279$, $R^2 = 0,99345$); for ΔH exponential regression was performed ($y = 27,959\ e\ 0,0347x$. $R^2 = 0,92439$). MMPs were ordered per molecular weight and divided into three groups: S_1 shallow (MMP-7), S_1 deep (MMP-3) and S_1 intermediate (MMP-8, MMP-2 and MMP-9), these structural features correlated to T_m and ΔH parameters.

Removal of the pro-peptide is required for MMP activation, resulting in protein conformational changes that can be detected by DSC. Gelatinases; ProMMP-9 and ProMMP-2, once activated, revealed a higher and lower temperature transitions, confirming that relevant conformational changes occurred after PD removal, even though the predicted structures show minor changes. The only data reported of calorimetric studies on MMP, corresponds to MMP-2 [31]. A thermal denaturation of this enzyme shows a single broad transition at T_m 72 °C, which is like the transition observed in this study for ProMMP-2, with T_m at 71.3 °C. The small difference between our results can be explained by an incomplete baseline subtraction done in the MMP-2 DSC analysis done in the referred study [31].

The fact that the catalytic domain of MMP-3, unfolds at T_m 83.4 °C, the same transition temperature for one of the components present in the active form of MMP-3 (T_m 83.9 °C), strongly suggests that they corresponded to the same structural domain. The conformation of the CD within the protein, is not affected after PD and HD removal.

To further support the idea that the CD in the rest of the MMP studied corresponded to the transition observed at higher T_m, the MMP-7, which it is only composed of the catalytic domain, had a single transition at T_m 98.3 °C. The high T_m and low enthalpy of rMMP-7 give this protein a restricted temperature range in which the native state of the protein is stable once the T_m is reached, implying that is structural conformation is one of the most stable among the MMP. Differential Scanning Calorimetry add further information on the role of conformational changes during MMP activation and substrate interaction. A restriction of DSC to analyse complex biological samples is the need for highly purified forms of the enzymes for DSC studies, a situation that could be overcome with the use of standardized values of thermal denaturation, such as those presented in this paper, as a reference to identify the specific contribution of enzyme domains in a complex mix of cellular products as it has been previously seen in chorioallantoid membrane during labour [2].

The fact that MMP catalytic domain has a very high T_m, which is not substantially affected after removal of the propeptide domain has provided us insight not only in the understanding of the conformational changes that occur under activation of the pro enzyme, but also give some indication to understand the mechanism of collagenolysis.

4. Experimental procedures

4.1. Reagents and antibodies

Human recombinant active (rMMP) and proenzymes (rPro-MMP) were purchased from Calbiochem (EMD Biosciences, SanDiego, CA) including active MMP-2 and proMMP-2, catalytic domain of MMP-3, active MMP-3 and proMMP-3, active MMP-7, active MMP-8, and active MMP-9 and, proMMP-9. Monoclonal antibodies against MMP-9 (Ab-3), MMP-8 (Ab-1), MMP-3 (Ab-1), were purchased from Calbiochem. Antibody against MMP-2 (Ab-11) was obtained from Pharmingen (BD Biosciences, San Jose, CA). For all MMPs the SDS-PAGE shows a single band except for MMP-9 where two bands were presents as indicated in the technical report.

4.2. Electrophoresis and immunoblotting

Protein content of rMMP was determined by Bradford assay per manufacturer's instructions (Sigma-Aldrich, St Louis, MO). Equal amounts of protein (0.5 μg/sample) were resolved on 10% sodium dodecyl sulphate polyacrylamide gel electrophoresis (SDS-PAGE) under reducing conditions and heated in a thermal cycler at a heating rate of 1ºC/min up to 95 °C. The SDS-PAGE was transferred to nitrocellulose membranes (Amersham Biosciences, NJ, USA). After several washes with PBST, the membranes were incubated with the appropriate secondary antibodies conjugated with horseradish peroxidase (goat anti-mouse 1:3000, BD Biosciences or goat anti-rabbit 1:40,000, Jackson Immunoresearch, WestGrove, PA, USA). Detection of complexes was performed using ECL per the manufacturer's recommendations (Amersham Biosciences, NJ, USA). Densitometry analysis was performed with UVP BioImaging System (UVP, Upland, CA). The relative abundance of MMP bands was determined by image analysis using arbitrary measures with UVP Bioimaging System (UVP, Upland, CA). Molecular weight (MW) of each band was calculated using protein standards (Invitrogen, Life Technologies, Inc. Carlsbad, CA, USA). Profile of MMP was determined by differential scanning calorimetry (DSC).

4.3. Differential scanning calorimetry (DSC)

A high-resolution Microcal VP-DSC (MicroCal LLC, Northampton, MA, USA) was used to obtain all scans. Recombinant proteins were diluted in a buffer containing: 0.1 M KCl, 0.02 M Tris-Maleate at pH 7.0, followed by overnight dialysis against the same buffer. Proteins and reference solutions were carefully degassed under vacuum for 5 min before loading the cells (0.56 ml). The unfolding profile of rPro-MMP-2, rPro-MMP-3 and rPro-MMP-9, and the rMMP active forms; rMMP-2, 3, 7, 8 and 9, were heated at a rate of 1 °C/min from 10 to 100 °C per established protocols [11, 13, 15]. Denaturation was completely irreversible after scanning up to 100 °C. DSC scans were deconvoluted assuming irreversible denaturation. The transition temperature (T_m) is defined as the temperature of half denaturation, and corresponds to the temperature at half the area under the individual peaks after the DSC scans were deconvoluted. This procedure requires that denaturation can be approximated by a two-state reaction of the form

$$N \xrightarrow{k} D$$

that obeys pseudo first-order kinetics, and where the temperature dependence of the rate constant k is given by the Arrhenius relation, as described previously [13, 15]. These assumptions have been shown to hold for the SERCA and PMCA enzymes in skeletal muscle [13, 14], several mammal tissues proteins [15] and for Colicines [16]. The fraction of each component denatured as a function of increasing temperature at a constant rate (f_D) is given as,

$$f_D[T(t)] = 1 - \exp\left\{ -\left(\frac{RT_c^2}{E_A v}\right)\exp\left(\frac{E_A(T - T_c)}{RT_c^2}\right)\right\}$$

where Tc is the temperature at which $k = 1$, t is time, and v is the scan rate. The derivative of f_D as a function of temperature is proportional to the excess C_p. The curves of excess C_p as a function of temperature were deconvoluted into individual components using a recursive minimization routine [13].

4.4 Protein Structure Predictions.Swiss-Model repository, a database of available annotated three-dimensional comparative protein structure models generated by fully automated homology-modelling pipeline from Swiss-model [32] (http://swissmodel.expasy.org/repository) and SwissPdb Viewer (http://expasy.org/spdbv7) were utilized for protein modelling of MMPs. For all cases, the NH2-terminal is oriented in the upper-right side of the molecule that corresponds to the catalytic Domain (CD) -labelled green-, the COOH-terminal which is oriented in the lower-right side of the molecule that corresponds to the hemopexin domain (HD)-labelled blue-, the propeptide domain (PD) -labelled red- and the fibronectin-like domain (FD) -labelled yellow.

Declarations

Author contribution statement

N. Meraz-Cruz: Conceived and designed the experiments; Performed the experiments; Analyzed and interpreted the data; Wrote the paper.

A. Ortega: Conceived and designed the experiments; Performed the experiments; Analyzed and interpreted the data; Contributed reagents, materials, analysis tools or data; Wrote the paper.

F. Vadillo-Ortega: Analyzed and interpreted the data; Contributed reagents, materials, analysis tools or data; Wrote the paper.

A. Jiménez-Garduño: Analyzed and interpreted the data; Wrote the paper.

Funding statement

F. Vadillo-Ortega was supported by Consejo Nacional de Ciencia y Tecnología, México (C01-7036). A. Ortega was supported by Universidad Nacional Autónoma de México (DGAPA-IN218215 and DGAPA-IN-IN219119).

Competing interest statement

The authors declare no conflict of interest.

Additional information

No additional information is available for this paper.

Acknowledgements

Funding for this project was obtained from CONACyT grant C01-7036, Consejo Nacional de Ciencia y Tecnología, Mexico (to F. Vadillo-Ortega), grants DGAPA-IN218215 and DGAPA-IN- IN219119 (Dirección General del Personal Académico, Universidad Nacional Autónoma de México (UNAM)) (to A. Ortega). We thank M.C. Ibrahim Ramirez for reviewing the manuscript.

References

[1] S.E. Ulbrich, S.U. Meyer, K. Zitta, S. Hiendleder, F. Sinowatz, S.M. Bauersachs, et al., Bovine endometrial metallopeptidases MMP14 and MMP2 and the metallopeptidase inhibitor TIMP2 participate in maternal preparation of pregnancy, Mol. Cell. Endocrinol. 332 (1-2) (2011) 48–57.

[2] N. Meraz-Cruz, A. Ortega, G. Estrada-Gutierrez, A. Flores, A. Espejel, C. Hernandez-Guerrero, F. Vadillo-Ortega, Identification of a Ca2+-dependent matrix metalloproteinase complex in rat chorioallantoid membrane during labour, Mol. Hum. Reprod. 10 (2016) 633–641.

[3] V.O. Maia-Filho, A.M. Rocha, F.P. Ferreira, T.C. Bonetti, P. Serafini, E.L. Motta, Matrix metalloproteinases 2 and 9 and e-cadherin expression in the endometrium during the implantation window of infertile women before in vitro fertilization treatment, Reprod. Sci. 22 (4) (2015) 416–422.

[4] L. Amar, S. Smith, G.B. Fields, Matrix metalloproteinase collagenolysis in health and disease, Biochem. Biophys. Acta 1864 (11PtA) (2017) 1940–1951.

[5] N. Cui, M. Hu, R.A. Khalil, Biochemical and biological attributes of matrix metalloproteinases, Prog. Mol. Biol. Transl. Sci. 147 (2017) 1–73.

[6] J. Vandooren, P.E. Van den Steen, G. Opdenakker, Biochemistry and molecular biology of gelatinase B or matrix metalloproteinase-9 (MMP-9): the next decade, Crit. Rev. Biochem. Mol. Biol. 48 (3) (2013) 222–272.

[7] Yoshifumi Itoh, Membrane-type matrix metalloproteinases: their functions and regulations, Matrix Biol. 44 (46) (2015) 207–223.

[8] J. Jaoude, Y. Koh, Matrix metalloproteinases in exercise and obesity, Vasc. Health Risk Manag. 12 (2016) 287–295.

[9] T.C. Appleby, A.E. Greenstein, M. Hung, A. Liclican, M. Velasquez, A.G. Villaseñor, et al., Biochemical characterization and structure determination of a potent, selective antibody inhibitor of human MMP9, J. Biol. Chem. 292 (16) (2017) 6810–6820, 2017.

[10] C.A. Galea, H.M. Nguyen, K.G. Chandy, B.J. Smith, D. Norton, Domain structure and function of matrix metalloprotease 23 (MMP23): role in potassium channel trafficking, Cell. Mol. Life Sci. 71 (2014) 1191–1210.

[11] P. Privalov, Scanning microcalorimetry in studying temperature induced changes in proteins, Methods Enzymol. 13 (1986) 4–51.

[12] S. Swarnakar, A. Mishra, S.R. Chaudhuri, The gelatinases and their inhibitors: the structure-activity relationships, Experientia Suppl. 103 (2012) 57–82.

[13] J.R. Lepock, K.P. Ritchie, M.C. Kolios, A.M. Rodahl, K.A. Heinz, J. Kruuv, Influence of transition rates and scan rate on kinetic simulations of differential scanning calorimetry profiles of reversible and irreversible protein denaturation, Biochemistry 31 (1992) 12706–12712.

[14] J.R. Lepock, Mesurement of protein stability and protein denaturation in cells using differential scanning calorimetry, Methods 35 (2) (2005) 117–125.

[15] A. Ortega, J.R. Lepock, Use of thermal analysis to distinguish magnesium and calcium stimulated ATPase activity in isolated transverse tubules from skeletal muscle, Biochem. Biophys. Acta 1233 (1) (1995) 7–13, 26.

[16] A. Ortega, S. Lambotte, B. Bechinger, Calorimetric investigations of the structural stability and interactions of colicin B domains in aquos solution and in the presence of phospholipid bilayers, J. Biol. Chem. 276 (2001) 13563–13572.

[17] J. Saus, S. Quinones, Y. Otani, H. Nagase, E.D. Harris Jr., M. Kurkinen, The complete primary structure of human matrix metalloproteinase-3. Identity with stromelysin, J. Biol. Chem. 263 (1988) 6742–6745.

[18] W. Yu, J.F. Woessner Jr., Heparan sulphate proteoglycans as extracellular docking molecules for matrilysin (matrix metalloproteinase 7), J. Biol. Chem. 275 (6) (2000) 4183–4191.

[19] S. Lenglet, F. Mach, F. Montecucco, Role of matrix metalloproteinase-8 in atherosclerosis, Mediat. Inflamm. (2013) 1–6, 2013; 659282.

[20] R. Swetha, C. Gayen, D. Kumar, T.D. Singh, S.K. Modil, Singh. Biomolecular basis of matrix metallo proteinase-9 activity, Future Med. Chem. 10 (9) (2018) 1093–1112.

[21] R. Fridman, M. Toth, D. Peña, S. Mobashery, Activation of progelatinase B (MMP-9) by gelatinase A (MMP-2), Canc. Res. 55 (12) (1995) 2548–2555, 1995 Jun 15.

[22] S.D. Shapiro, C.J. Fliszar, T.J. Brockelmann, R.P. Macham, R.M. Senior, H.G. Welgus, Activation of the 92-kDa Gelatinase by Stromelysin and 4-Amino-phenylmercuric Acetate. Differential processing and stabilization of the carboxyl-terminal domain by tissue inhibitor of metalloproteinases (TIMP), J. Biol. Chem. 270 (11) (1995) 1651–1656.

[23] B.S. McCrary, S.P. Edmondson, J.W. Shriver, Hyperthermophile protein folding thermodynamics: differential scanning calorimetry and chemical denaturation of Sac7d, J. Mol. Biol. 264 (1996) 784–805.

[24] H.I. Park, Y. Jin, D.R. Hurst, C.A. Monroe, S. Lee, M.A. Schwartz, Q.-X.A. Sang, The intermediate S1 pocket of the endometase/matrilysin-2 active site revealed by enzyme inhibition kinetic studies, protein sequence analyses, and homology modeling, J. Biol. Chem. 278 (51) (2003) 51646–51653.

[25] T. Duellman, S. Burnett, J. Yang, Functional roles of N-linked glycosylation of human matrix metalloproteinase 9, Traffic 16 (10) (2015) 1108–1126.

[26] Y. Okada, Y. Gonoji, K. Naka, K. Tomita, I. Nakanishi, K. Iwata, et al., Matrix metalloproteinase 9 (92-kDa gelatinase/type IV collagenase) from HT 1080 human fibrosarcoma cells. Purification and activation of the precursor and enzymatic properties, J. Biol. Chem. 267 (30) (1992) 21712–21719.

[27] C. Park, M.J. Lee, J. Ahn, J.S. Kim, H.H. Kim, K.H. Kim, et al., Heat shock-induced matrix metalloproteinase (MMP)-1 and MMP-3 are mediated through ERK and JNK activation and via an autocrine interleukin-6 loop, J. Invest. Dermatol. 123 (6) (2004) 1012–1019.

[28] J.R. Lepock, How do cells respond to their thermal environment? Int. J. Hyperther. 21 (8) (2005) 681–687.

[29] Y. Matsuura, T. Takehira, Y. Joti, K. Ogasahara, et al., Thermodynamics of Protein Denaturation at Temperaturesover 100 °C: CutA1 Mutant Proteins Substituted with Hydrophobic and Charged Residues, Scientific Report, Open Access, 2015.

[30] A. Ortega, V.M. Becker, R. Alvarez, J.R. Lepock, H. Gonzalez-Serratos, Interaction of D-600 with the transmembrane domain of sarcoplasmic reticulum Ca2+-ATPase, Am. J. Physiol. 279 (2000) 166–172.

[31] L. Banayai, H. Tordai, L. Patthy, Structure and domain-domain interactions of the gelatine-binding site of human 72-KD type IV collagenase (Gelatinase A, Matrix Metalloproteinase 2), J. Biol. Chem. 271 (20) (1996) 12003–12008.

[32] J. Kopp, T. Schwede, The SWISS-MODEL Repository of annotated three-dimensional protein structure homology models, Nucleic Acids Res. 32 (2004) D230–D234.